Series of Exon-Skipping Events in the Elastic Spring Region of Titin as the Structural Basis for Myofibrillar Elastic Diversity

Alexandra Freiburg, Karoly Trombitas, Wolfgang Hell, Olivier Cazorla, Françoise Fougerousse, Thomas Centner, Bernhard Kolmerer, Christian Witt, Jaques S Beckmann, Carol C Gregorio, et al.

Series of Exon-Skipping Events in the Elastic Spring Region of Titin as the Structural Basis for Myofibrillar Elastic Diversity

Alexandra Freiburg,† Karoly Trombitas, Wolfgang Hell, Olivier Cazorla, Francoise Fougerousse, Thomas Centner, Bernhard Kolmerer, Christian Witt, Jaques S. Beckmann, Carol C. Gregorio, Henk Granzier, Siegfried Labeit

Abstract—Titins are megadalton-sized filamentous polypeptides of vertebrate striated muscle. The I-band region of titin underlies the myofibrillar passive tension response to stretch. Here, we show how titins with highly diverse I-band structures and elastic properties are expressed from a single gene. The differentially expressed tandem-Ig, PEVK, and N2B spring elements of titin are coded by 158 exons, which are contained within a 106-kb genomic segment and are all subject to tissue-specific skipping events. In ventricular heart muscle, exons 101 kb apart are joined, leading to the exclusion of 155 exons and the expression of a 2.97-MDa cardiac titin N2B isoform. The atria of mammalian hearts also express larger titins by the exclusion of 90 to 100 exons (cardiac N2BA titin with 3.3 MDa). In the soleus and psoas skeletal muscles, different exon-skipping pathways produce titin transcripts that code for 3.7- and 3.35-MDa titin isoforms, respectively. Mechanical and structural studies indicate that the exon-skipping pathways modulate the fractional extensions of the tandem Ig and PEVK segments, thereby influencing myofibrillar elasticity. Within the mammalian heart, expression of different levels of N2B and N2BA titins likely contributes to the elastic diversity of atrial and ventricular myofibrils.

Key Words: atrium ■ titin ■ elasticity ■ diastole

In addition to the active muscle force, myofibrils also generate passive forces when stretched above or shortened to below the slack length. Passive forces are directed to restore thick and thin filament overlap at rest; ie, vertebrate myofibrils have an intrinsic elasticity that is independent from the active force generating crossbridges. This elastic force resides within a third filament system, which is formed by titin. The giant polypeptide chain of titin is ≈3 MDa in size, and in situ it spans from Z- to M-lines, a distance of 1 to 2 μm (for reviews on titin elasticity, see References 1 and 2). During physiological amounts of myofibril stretch, ≈90% of the elastic passive tension response of cardiac muscle is derived from the titin filament system, whereas particularly in the heart muscle, collagen and intermediate filaments become important when preventing further nonphysiological overstretch.[3]

Three different sequence elements account for the extensibility of the I-band region of titin. One spring element is composed of tandemly arranged Ig domains. This element extends 3- to 4-fold at low forces, presumably by unbending interdomain linkers, whereas the Ig domains themselves maintain their tertiary structures.[4,5] A second spring element, referred to as the PEVK segment, is formed by a sequence region rich in proline (P), glutamine (E), valine (V), and lysine residues (K).[6] The PEVK spring produces most of the physiological passive tension response of titin, presumably by functioning as an entropic spring. Finally, the so-called N2B sequence of cardiac titin extends toward the end of the physiological sarcomere length (SL) range. In situ, the tandem Ig, PEVK, and N2B segments act as a serially linked multiple-spring system with elements that are sequentially recruited during stretch.[7–9]

The elastic properties of myofibrils from different vertebrate species and tissues are highly divergent, reflecting functional specialization. Tissue-specific expression of titin isoforms with different elasticities was suggested by gel-electrophoretic and sequencing studies.[6,10–12] However, details of how muscles express highly diverse titins are unclear. Here, we determined the human gene sequence of titin that codes for its elastic I-band region. Characterization of titin transcripts from cardiac and skeletal muscles shows that cascades of exon-skipping events produce titins with distinct

From the European Molecular Biology Laboratory (A.F., T.C., B.K., S.L.), Heidelberg, Germany; Institut für Anästhesiologie und Operative Intensivmedizin (A.F., C.W.), Universitätsklinikum Mannheim, Germany; Department of Veterinary and Comparative Anatomy, Pharmacology, and Physiology (K.T., O.C., H.G.), Washington State University, Pullman, Wash; Medigenomix (W.H.), Martinsried, Germany; Genethon (F.F., J.B.), Evry, France; and the Department of Cell Biology and Anatomy (C.C.G.), University of Arizona, Tucson, Ariz.

†Deceased.

Correspondence to Dr Siegfried Labeit, EMBL, Meyerhofstrasse 1, 60012 Heidelberg, Germany. E-mail labeit@embl-heidelberg.de

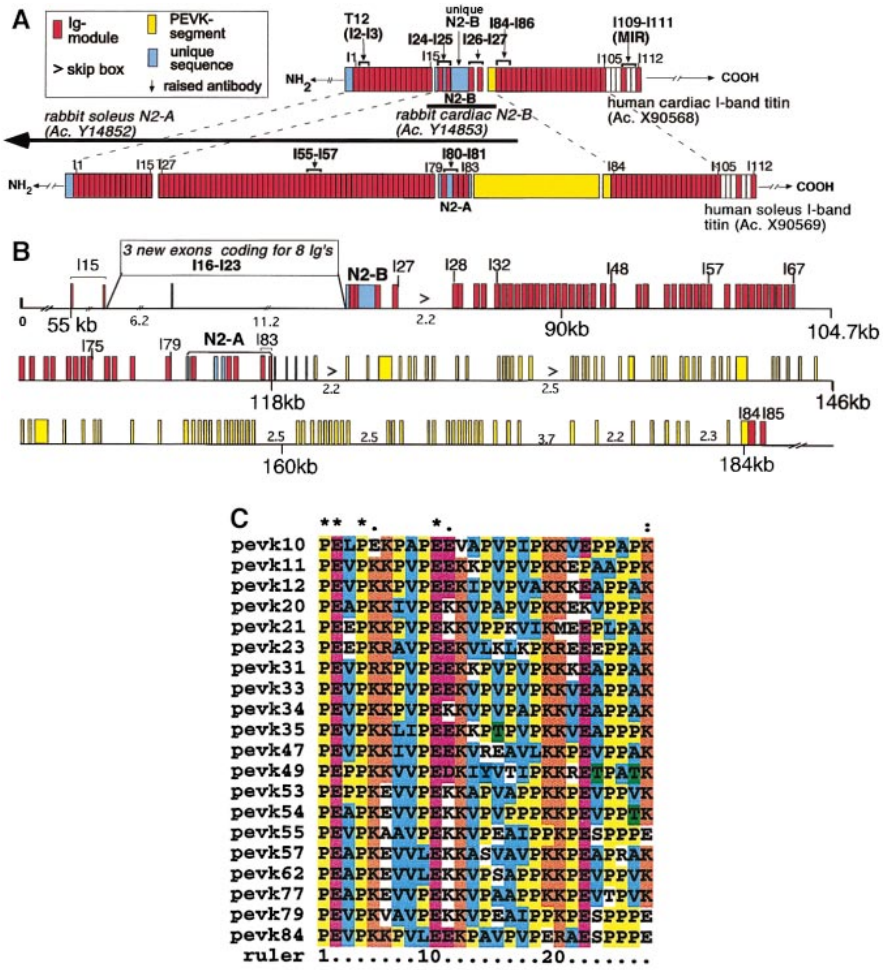

Figure 1. The differentially expressed I-band segment of titin. A, Titin cDNAs from cardiac muscle (top) and soleus skeletal muscle (bottom) predict titins that have very different I-band regions. Antibodies were raised for immunofluorescence/immunoelectron microscopy studies, and their epitopes are indicated by arrows; the monoclonal antibody T12 is directed to I2/I3; anti-MIR is directed to the main immunogenic region in titin (I109 to I111). In skeletal muscle, 4 of these antibodies mark the proximal and distal tandem Ig segments and the PEVK segment. Anti-N2B antibodies detect heart-specific N2B epitopes. Rabbit cDNAs determined for RT-PCR studies are indicated by thick lines. Ac. indicates EMBL accession number. B, Genomic organization within the differentially expressed I15-to-I84 130-kb region. C, Comparison of the 80- to 90-nucleotide PEVK exons reveals a family of conserved 26- to 30-residue PEVK repeats.

I-band structures and that myogenic differentiation results in muscle types with unique titin-based elastic properties.

Materials and Methods

Sequence Data

The 106-kb human titin gene sequence spanning from I24 to I84 is available from the European Molecular Biology Laboratory data library (EMBL), accession No. AJ277892; the rabbit titin soleus and cardiac N2B cDNA sequences are under accession Nos. Y14852 and Y14853.

Isoform Transcript Studies

RNAs from different rabbit muscles were analyzed by reverse transcriptase–polymerase chain reaction (RT-PCR) with combinations of I15S-to-I84R primers. cDNA clones were isolated from human adult heart, human skeletal leg muscle, and rabbit skeletal psoas muscle cDNA libraries with N2B/N2A probes. Human fetal embryos (age from 4 to 7 postovulatory weeks) were from legal abortions induced by mifepristone (RU486), approved by the Ethical Committee Necker Hospital Paris. In situ hybridization probes were chimeric 30-meric antisense oligonucleotides of which the 15 5′ base pairs were from the donor and the 15 3′ bases were from the acceptor exon.

Antibodies, SDS-PAGE, and Western Blot Analysis of Titin

For origin of the titin antibodies used and gel electrophoresis and Western blot conditions, see online Materials and Methods (http://www.circresaha.org). For epitope locations, see Figure 1.

Passive Tension Measurements

Cardiac myocytes were from rat (male Sprague-Dawley, 250 g) or pig (Yorkshire-type swine, 20 to 30 kg). For myofibril attachment and passive tension measurements, see online Materials and Methods (http://www.circresaha.org).

Immunoelectron and Immunofluorescence Microscopy

Skeletal muscle fibers and cardiac cells were stretched, fixed, immunolabeled, embedded, and processed for electron microscopy, as described online (http://www.circresaha.org). Indirect immunofluorescence microscopy of 8- to 10-μm frozen sections of rat (n=5) and rabbit (n=2) ventricular and atrial myocardium and pig ventricular myocardium (n=2) was essentially as described.[8]

An expanded Materials and Methods section is available online at http://www.circresaha.org.

Results

A 106-kb Genomic Region Codes for the Differentially Expressed Spring Families of Titin

Two sequenced titin isoforms from human myocardium and human soleus skeletal muscle cDNA libraries, referred to as N2B and N2A titins, have homologous A-band but strikingly different I-band regions (Figure 1).[6] To investigate the molecular basis of titin diversity, we determined the human gene sequence of titin within the differing N2A/N2B/PEVK regions (for details, see online Materials and Methods [http://www.circresaha.org]). Within the PEVK region, the gene

sequence indicates the presence of at least 27 novel exons that are not included in the cardiac and skeletal titin cDNA sequences (Figure 1A). Twenty-five of the novel PEVK exons are 80 to 89 bp in length and highly homologous to each other and code for ≈27-residue PEVK elements (Figure 1B). Two new exons 5′ of N2B together code for 8 novel Ig repeats. Previously, we named Ig repeats by counting them in human cardiac titin.[6] The discovery of novel titin I-band Ig repeats interferes with this terminology. Below, we refer to individual I-band Ig repeats by counting them from 5′ to 3′ (N to C terminally) in the gene sequence. On the basis of this system, the differentially spliced region spans I15 to I84 and encompasses 161 exons (Figure 1). In the N2B heart isoform, 155 exons are skipped by splicing together the I27 and PEVK exons, which are 101 kb apart (Figure 1). The N2B segment is coded for by a single 2.7-kb exon containing repeats I24/I25/I26. The N2A segment containing I80 to I83 is coded for by a group of 6 exons 35 kb farther downstream (Figure 1A).

Different Exon-Skipping Pathways Produce N2A, N2B, and N2BA Titins

To study the tissue-specific splicing of the titin gene in an animal model, we amplified cDNAs from 12 different rabbit muscles with I15S-to-I84R primer pairs. The N2A exons are expressed in all striated muscles (Figure 2A). In skeletal muscles, the N2B exon is excluded by splicing together I15/I27 (Figure 2A), whereas inclusion of N2B is obligatory in the adult heart (Figure 2B). To further characterize N2B cardiac titin(s), I27S together with I28R-to-I84R primers was tested for amplification of rabbit cardiac cDNAs. I27S+I84R amplified a "minimal-size" N2B titin isoform in which the Ig repeats I28 to I83 and 92% of the N-terminal PEVK domain are excluded. Further cardiac isoforms were amplified with I27S+I61R and I27S+I82R, which contain both the N2A and N2B elements but differ by multiple skipping variants in the I27-to-I68 segment (Figures 2B and 3). The exon skips within I27 to I68 varied in different anatomical regions of the rabbit heart (Figure 2B). In human, multiple variants were also identified in the I27-to-I68 segment when clones were selected by conventional filter screens with I27-to-I84 probes. Extensions to the 3′ end with I79S identified a 600-residue human PEVK domain isoform that is derived from the full-length soleus PEVK by a complex series of skipping events (Figure 3). Finally, RT-PCR analysis of rabbit skeletal muscles showed that only soleus muscle expresses I27 to I34 as a continuous fragment, whereas all other tested striated muscles skip I30 to I34. For example, psoas muscle skips I30 to I47 (Figures 2A and 3). During development, in situ hybridizations of human fetal sections with titin anti-sense oligonucleotides directed to the N2B-to-I27 and I27-to-I68 junctions show that these splice routes are specific to the heart at week 10 (Figure 2C). Therefore, yet unknown factors determine the tissue specificity of titin splice routes during early development.

In summary, skeletal titin transcripts are N2A based (ie, they always include the N2A segment and exclude the N2B exon), whereas cardiac titins are N2B based (ie, cardiac titins always include the N2B exon). Furthermore, in heart, very different splice routes for titin coexist. One major cardiac splice route

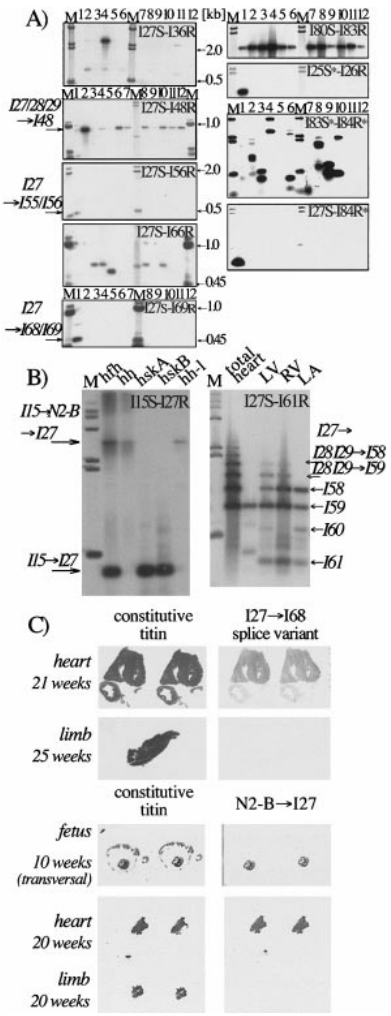

Figure 2. Exon-skipping events in titin. A, Left, RT-PCR analysis of rabbit striated muscles within the central I-band region. Location of primer pairs indicated at top right. Lane M, λ *Hin*dIII size marker; lane 1, heart left ventricle; lane 2, M. psoas; lane 3, M. longissimus dorsi; lane 4, M. soleus; lane 5, M. gastrocnemius; lane 6, M. plantaris longus; lane 7, diaphragm; lane 8, M. extensor digitorum longus; lane 9, M. tibialis anterior; lane 10, M. rectus femoris; lane 11, tongue; lane 12, M. pectoralis major. Tissue-specific exon skips occur in the proximal tandem Ig segment. A contiguous I27-to-I36 segment is expressed only in soleus muscle. Skipping of I28 to I47, I28 to I54, and I28 to I67 occurs in psoas (lane 2) and heart muscle (lane 1). A, Right, I80 to I83 (N2A segment) is expressed in all striated muscles, whereas expression of I24 to I26 (N2B exon) is restricted to cardiac muscle. B, Left, PCR amplification of total human cDNAs from fetal cardiac (hfh), adult cardiac (hh), and skeletal adult (hskA and hskB) muscles with N2B flanking I15S+I27R primers. Skeletal muscles join exons I15 to I27, whereas cardiac adult muscle includes N2B exonic I24/I25/I26 between I15 and I27. In human fetal heart (week 20), N2B including and excluding splice routes coexists (hh-1, control template of a sequenced cardiac cDNA clone). B, Right, Multiple N2B-based cardiac isoforms result from joining I27 to acceptors in I28 to I68. Arrows/labels indicate the respective Ig repeats joined by splicing. LV indicates left ventricle; RV, right ventricle; LA, left atrium. C, In situ hybridization of fetal human sections. Antisense probes complementary to I26/I27 and I27/I68 junctions (right) stain specifically the developing heart, whereas the constitutive control probe from the M-line titin region also stains the surrounding body wall muscles (week 10, left) and limb muscles (weeks 10 and 20).

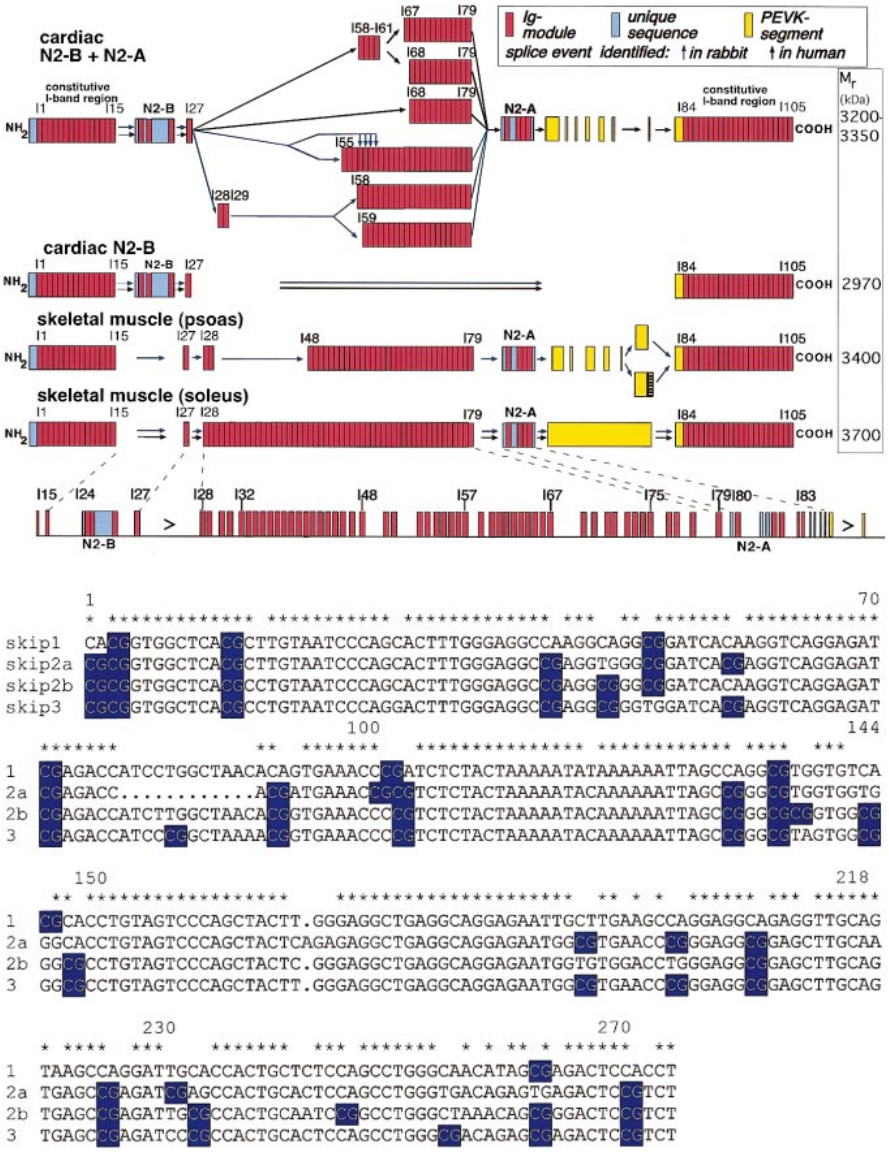

Figure 3. Top, Overview of differential splice pathways in the I15-to-I84 region. Identified splice routes are indicated by arrows, black for human and blue for rabbit. Predicted molecular weights of respective isoforms are given (right). All isoforms share the I27 exon, and tissue-specific variants derive 5′ and 3′ of this exon. Bottom, Sequence homology of the intron 3′ to I27 and 2 introns from the PEVK region. Note the frequency of CpG pairs (blue).

joins the I15-to-I24/I27-to-I84 exons and therefore is predicted to express a small cardiac titin (N2B titin with 2.97 MDa). A second pathway includes both the N2A and N2B segments, plus 12 to 25 tandem Ig repeats (I55 to I79) and a ≈600-residue-long PEVK domain (cardiac N2BA titin with a predicted 3.3 MDa). In psoas and soleus skeletal muscles, distinct splice pathways produce cDNAs coding for larger titin isoforms (3.4 MDa in psoas and 3.7 MDa in soleus). All titin isoforms identified so far share the I27 exon, and much of the isoform diversity of titin results from its differential splicing to multiple downstream acceptor exons within I28 to I84 (Figure 3). Interestingly, the intron 3′ to I27 shares extensive sequence homology with 2 introns from the differentially spliced PEVK region, raising the possibility that conserved intron motifs are implicated in exon skipping (Figure 3).

Differentially Processed Titin Transcripts Translate Into Titin Isoforms

If many structurally different titins are expressed, this complicates how proper stoichiometry and assembly into sarcomeres could be achieved. Therefore, we tested whether titin splice isoforms translate into distinct polypeptides. In agreement with earlier studies, low-percentage SDS gradient gels detect differently sized titins in soleus, psoas, and heart muscle (Figure 4A, see also References 10–12). Western blot analysis with anti-I55/I56/I57, anti-N2A-to-I80/I81, and anti-N2B antibodies shows that skeletal titins are N2A based (Figure 4B), whereas cardiac titins are N2B based (Figure 4C). Different titin size classes are detected in myocardium of some species. Myocardium of all investigated species contains a major T1 band with the same mobility, and an additional lower-mobility band is found in some of the investigated species. This additional band is present at low levels in rabbit and high levels in pig and human, whereas the band cannot be detected in rat myocardium (Figure 4A, middle and right panels). The lower-mobility band reacts with all tested antibodies (anti-I80/I81 [N2A], anti-N2B, and anti-I55/I56/I57 antibodies), whereas the higher-mobility band reacts only with anti-N2B antibodies (Figure 4C). These results suggest that the lower-mobility band corresponds to an

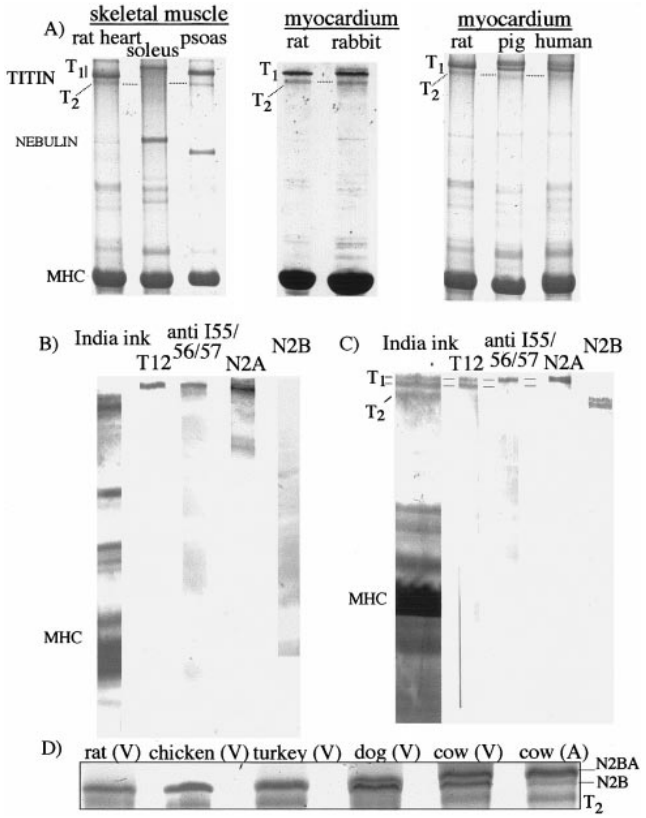

Figure 4. SDS-PAGE analysis of titin isoform expression in skeletal and heart muscles. A, Undegraded titin (T1 species) from rabbit psoas muscle migrates faster than rat soleus titin, consistent with the splice data (3.3 and 3.7 MDa in psoas and soleus, respectively). Pig and human left ventricular myocardium contain 2 T1 bands; the lower-mobility band is minor in rabbit and absent in rat left ventricular myocardium. Rat myocardium was included as a reference. B and C, Western blots with N2A- and N2B-specific antibodies using human soleus skeletal muscle (B) and human myocardium (C). Skeletal titin is N2A based. Human myocardium (C) contains 2 T1 bands. The bottom band reacts only with N2B antibodies, indicating that it represents the short N2B cardiac isoform. The top T1 band reacts with all tested antibodies, indicating that it represents the long N2BA cardiac isoform. D, Comparative gel electrophoresis of left ventricular (V) and atrial (A) myocardium from various species. See text for details.

N2BA titin isoform, whereas the higher-migrating band is an N2B titin. Comparison of cardiac titins from ventricles and atria of different species suggests the coexpression of variable amounts of N2B and N2BA titins (Figure 4D and Reference 13). Avian (chicken and turkey) myocardium expresses a single titin band that has a mobility similar to that of rat N2B titin, presumably representing N2B titin as well. Ventricular myocardium from dog and cow expresses high levels of a low-mobility titin that most likely represent N2BA titin. When comparing ventricular and atrial myocardium, N2BA titin is more abundant in the atrial tissue (Figure 4D). The 2 distinct cardiac size classes differentially reacting with anti-I55/I56/I57 and with anti-I80/81-N2A antibodies (Figure 4) is consistent with the coexpression of N2B and N2BA titins in the heart (Figure 3). These 2 isoforms are expressed at different levels in different species, and at different levels in atrial and ventricular myocardium.

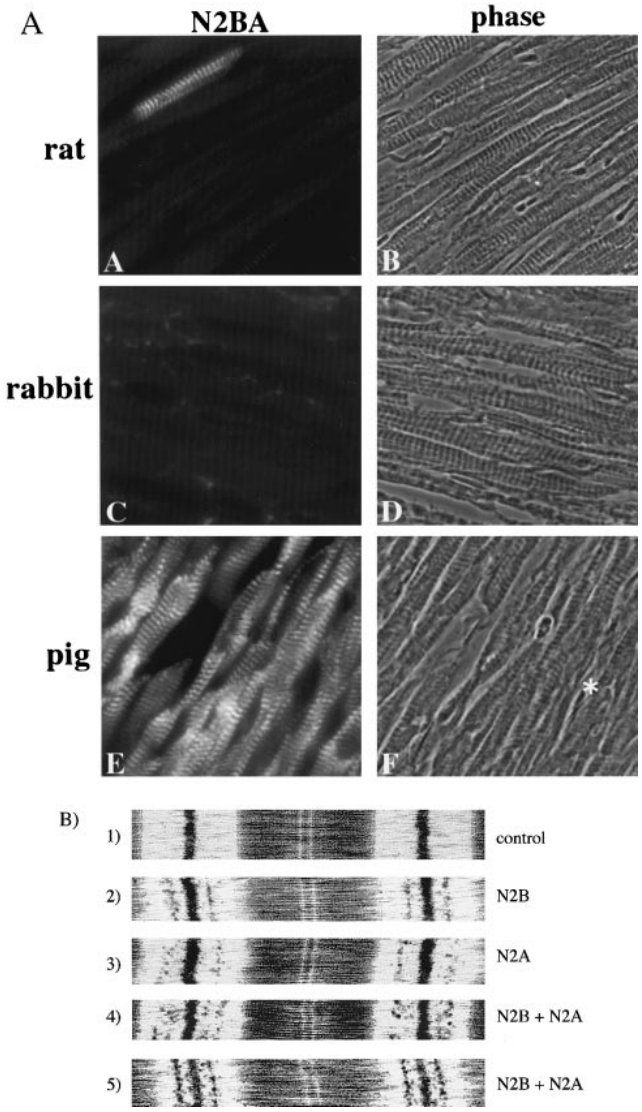

Figure 5. A through F, Immunofluorescence localization of the large N2BA titin isoform on frozen sections of rat, rabbit, and pig myocardium using anti-I53/54/55 antibodies. Staining is detected in a small subset of cardiac myocytes in rat (A, 1 random positive cell in this micrograph), rabbit (C, no positive cells in this micrograph), and most cardiac myocytes in pig (E; see asterisk in panel F for random cell not demonstrating staining). Note corresponding phase-contrast images (B, D, and F) to identify striated muscle tissue. Bar=10 μm. Bottom, B-1 through B-5, Immunoelectron microscopy on human myocardium using N2B and N2A antibodies. B-1, Control sarcomere (no primary antibody). B-2 and B-3, Sarcomeres labeled by N2B and N2A antibodies, respectively. Note epitope in middle of I-band. B-4 and B-5, Sarcomeres labeled simultaneously with both N2B and N2A antibodies. B-4, Example of a sarcomere containing 2 epitopes. B-5, Sarcomere containing 1 epitope only. Bar=0.5 μm.

Immunostaining with anti-I55/56/57 antibodies (recognizing the large N2BA titin isoform) detect this isoform in a subset (which appear to be randomly distributed) of cardiac myocytes. The frequency of expressing cells varied between species, ranging from a few percent in rat (1±1.4%) (Figure 5A) and rabbit (2.8±3.1%) (Figure 5C) to abundant I55/I56/I57 expression in pig (91±9.7%) (Figure 5E) and human myocardium (not shown). In immunoelectron microscopy, both the anti-I24/I25 (N2B) and anti-I80/I81 (N2A) antibod-

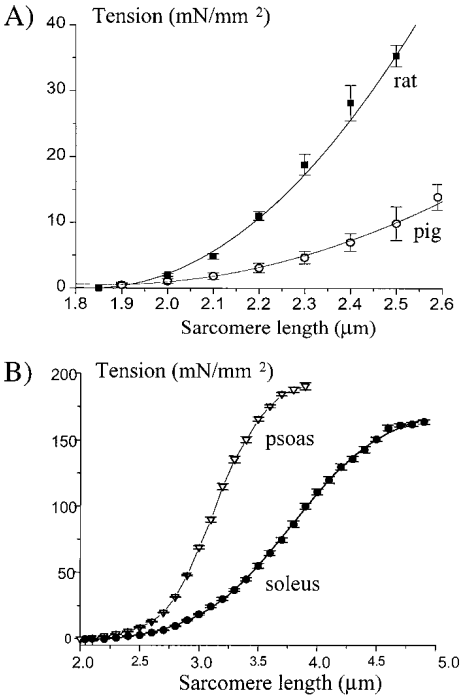

Figure 6. Passive tension of cardiac myocytes and skeletal muscle fibers. A, Passive tension–SL curves of rat ventricular cells (n=9 cells) and pig atrial cells (n=8 cells). At a given SL, rat cells develop severalfold higher passive tensions than pig cells. B, Passive tension–SL curves of rabbit psoas (n=4 fibers) and rabbit soleus (n=5 fibers) single fibers. Psoas fibers develop much higher levels of passive tension than soleus fibers. Data are mean±SEM.

ies label close to the middle of the I-band region of the sarcomere (Figures 5B-2 and 5B-3). The N2B epitope was on average closer to the Z-line than the N2A epitope. For example, at an SL of 2.4 μm, the epitope distance to the middle of the Z-line was 153±12 nm (n=6) for the N2B epitope and 270±30 nm (n=7) for the N2A epitope. When the tissue was double labeled with both N2B and N2A antibodies, the labeling pattern varied and sarcomeres were found with 2 epitopes (Figure 5B-4), as well as sarcomeres that contained a single epitope only (Figure 5B-5). When a single epitope was found, the distance to the Z-line suggested that it was derived from the N2B antibody and that the N2A epitope was absent. These results are consistent with the coexpression of structurally different N2B and N2BA titins in human myocardium.

I-Band Titin Isoform Type and Passive Force Generation

Cardiac myocytes were isolated from rat and pig myocardium, as these species represent examples of those that express high levels of N2B titin (rat) and high levels of N2BA titin (pig). Results indicate that passive tension of rat myocytes increases much more steeply with SL than that of pig myocytes (Figure 6A). Thus, the expression of N2B cardiac titin is associated with a high passive tension–generating ability.

The passive properties of muscle fibers isolated from rabbit soleus and psoas muscle were also studied. In sarcomeres longer than ≈2.5 μm, passive tension was found to increase much more steeply with SL in psoas than in soleus fibers (Figure 6B). To explore the origin of this, the lengths of the tandem Ig and PEVK segments were measured by immunoelectron microscopy (for examples of labeled sarcomeres, see Figure 7A). The lengths of these segments were measured in sarcomeres stretched to different lengths, and the segment lengths were expressed as a fraction of their contour length (for technical details see online Materials and Methods; http://www.circresaha.org). Results indicate that the fractional extension of tandem Ig and PEVK segments in sarcomeres shorter than ≈2.5 μm are similar in psoas and soleus fibers. However, at longer SLs the fractional extensions increase more steeply in psoas than in soleus fibers (Figures 7B and 7C). The significance of these findings is discussed below.

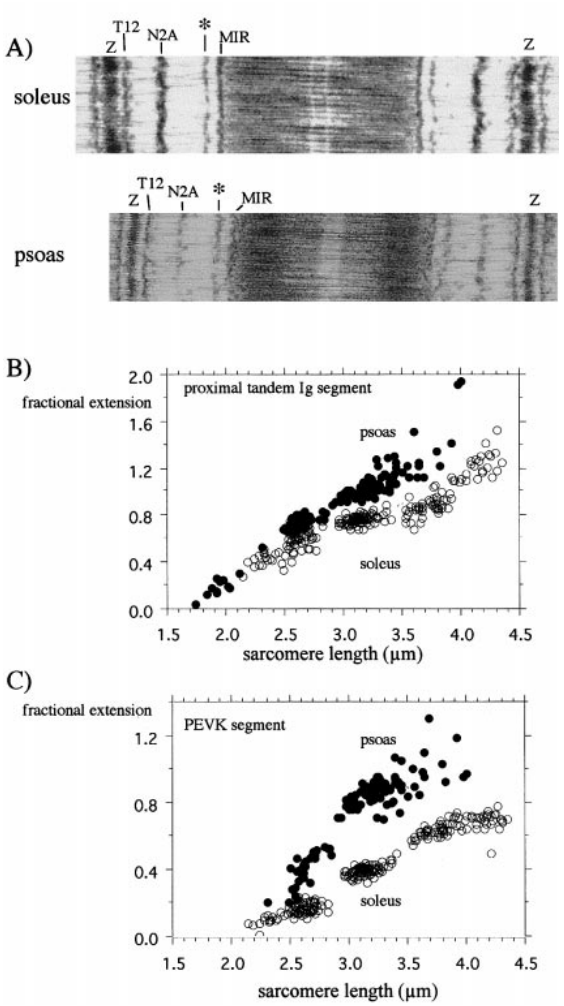

Figure 7. Extensibility of tandem Ig and PEVK segments of rabbit soleus and psoas muscle fibers. A, Examples of sarcomeres labeled by T12 (anti-I2/I3), N2A (anti-I80/I81), anti-I84/I85/I86 (marked with an asterisk [*]), and anti-MIR (raised to I109/I110/I111). Top, Soleus sarcomere. Bottom, Psoas sarcomere. Antibodies demarcate the tandem Ig and PEVK segments. B and C, Fractional extension–SL relations. Segment lengths were measured and divided by their contour length to obtain the fractional extension (contour lengths of tandem Ig, 330 nm [soleus] and 240 nm [psoas]; contour length of PEVK segment, 820 nm [soleus] and 350 nm [psoas]). In sarcomeres longer than ≈2.5 μm, fractional extension of tandem Ig and PEVK segments is higher in psoas than in soleus fibers. (Fractional extensions of tandem Igs that exceed 1.0 most likely result from unfolding of Ig domains.)

Discussion

The titin isoform family is encoded by a single gene located on chromosome 2, region 2q31, and its locus is part of a group of genes that maintained conserved syntenic order since the divergence of rodents and humans.[14] This study indicates that extensive exon shuffling in the I-band region of titin generates its isoform diversity, which is in charge of myofibrillar elastic diversity. Some of the splice pathway choices occur early and irreversibly during myogenesis, such as the cardiac-specific inclusion of the N2B exon (Figure 2). Other aspects of titin splice regulation, such as the myocardial N2B/N2BA isoform ratio, appear to be controlled more flexibly, because different amounts of N2B and N2BA titin isoforms are found in different compartments of the heart (Reference 13 and the present study). From the large number of titin splice isoforms in different muscle types suggested by RT-PCR experiments, we focused on defining the titin splice routes in 3 muscle types that have different elastic properties: skeletal soleus, psoas, and heart muscle. The soleus muscle expresses the largest titin isoform observed so far (3.7 MDa), whereas psoas muscle expresses a smaller titin (3.35 MDa) with shorter proximal tandem Ig and PEVK segments. In the heart, titin transcripts are processed by 2 distinct splice routes that lead to N2B and N2BA titins (2.97 and 3.3 MDa, respectively). Interestingly, the lengths of the tandem Ig and PEVK domains appear to correlate in the isoforms, which appears to require a coordination of their splicing within a 100-kb genomic segment. It remains to be seen whether the conserved introns in the tandem Ig and the PEVK regions participate in exon skip regulation and whether they provide a basis for tandem-Ig/PEVK splice coordination.

So far, individual Ig/FN3 repeats in titin were numbered on the basis of their location in the cardiac isoform.[6] For the repeats in the extensively spliced I-band region, it is now difficult to use this numbering consistently. Moreover, the titin gene codes for additional Ig repeats of yet-unknown function and tissue expression. Therefore, we propose to identify Ig repeats in the I-band by counting them from 5′ to 3′ in the human gene sequence. This nomenclature would allow for the systematic naming of the numerous splice pathways on the basis of the repeats that are spliced together (ie, I27-to-I84 splice pathway for the small cardiac N2B isoform, and I27 to I55 for the large cardiac N2BA isoform).

Tissue-specific variation in passive mechanical properties has been reported in many previous studies. They concluded that passive cardiac myocytes are much stiffer than passive skeletal muscle fibers, and that among different skeletal muscles, psoas muscle fibers are relatively stiff.[2,13,15,16] Our work extends these earlier findings. We found that passive tension increase is steeper with SL in psoas than in soleus fibers. Also, the passive tension increase is steeper in myocytes isolated from rat myocardium, which express predominantly the small N2B isoform, than in myocytes isolated from pig myocardium, which express high levels of the large N2BA isoform. The differences in tandem Ig and PEVK segment length of the different muscle types provide a molecular framework to understand these mechanical differences.

The effect of tandem Ig and PEVK segment lengths on passive force can be evaluated by considering the molecular mechanism of passive force generation. A passive model has emerged recently in which the tandem-Ig segments (containing folded Ig domains) and the PEVK segment (acting largely as an unfolded polypeptide) behave as serially linked entropic springs.[7–9] In short sarcomeres, these springs are in a contracted state with high entropy. On sarcomere extension the springs straighten, lowering their conformational entropy and resulting in a force, known as entropic force. This force increases with the fractional extension of the segment (end-to-end length divided by the contour length). The serially linked entropic springs model of passive force development may be applied to titin isoforms by adapting the entropic forces to the fractional extensions multiplied by the contour lengths of the tandem Ig and PEVK segments of the isoform. Contour lengths of tandem Ig and PEVK segments of psoas titin are ≈100 and ≈400 nm shorter, respectively, than in soleus titin, assuming a 5-nm repeat per Ig domain and 3.8 Å per PEVK residue. Thus, for a given SL the fractional extension will be higher in psoas that in soleus muscle (Figures 7B and 7C). It follows that entropic force is predicted to be much higher in psoas than in soleus fibers, consistent with the measured passive tension differences (Figure 6B). A similar analysis can be applied to the cardiac isoforms. The contour lengths of tandem Ig and PEVK segments are ≈100 and ≈200 nm shorter, respectively, in N2B than in N2BA titin. Thus, at a given SL the fractional extension of tandem Ig and PEVK segments is considerably higher for N2B titin than for N2BA titin and, therefore, passive force will be higher. This prediction is qualitatively unaffected by the N2B sequence, which all cardiac titin isoforms share. Thus, the serially linked entropic springs model predicts that the passive force–SL relation increases more steeply for cells containing high levels of N2B titin (rat) than for cells containing high levels of N2BA titin (pig). Consistent with the predicted differences, rat myocytes generate higher passive forces than pig myocytes (Figure 6A).

In conclusion, this work provides a molecular basis for understanding the diversity in passive mechanical properties of muscle. Plasticity in splicing in the I15-to-I84 segment results in isoforms that vary in contour length. As a result, the fractional extension–SL relation of different isoforms differs, and this gives rise to distinctly different passive force–SL relations. Thus, the differential expression of the spring region of titin presents a striking example of how titin elasticity is modulated by splicing. Possibly, splice plasticity may also allow functional adaptations of the titin springs in training or muscle disease. Future studies are warranted to identify the factors in charge of titin splice choices and how their action may be regulated by muscle function and pathology.

Acknowledgments

We gratefully acknowledge the support of the Deutsche Forschungsgemeinschaft (Grant La 668/6-1 to S.L.), the American Heart Association (Grant 98-WA-115 to O.C.), the NIH (Grants HL61497 and HL62881 to H.G. and HL57461 and HLO3985 to C.C.G.), the AFM (to J.B. and F.F.), and the HFSP (to S.L. and C.C.G.). We thank M. Vekemans and T. Attie from the Hopital Necker-Enfants

Malades for provision of the embryonic tissues and M. Greaser (Wisconsin University) for communication of results on the 28–amino acid residue repeats in the PEVK.[17] This work is dedicated to the memory of Alexandra Freiburg (9/10/72-7/14/99). We all miss her.

References

1. Erickson HP. Stretching single protein molecules: titin is a weird spring. *Science*. 1997;276:1090–1092.
2. Linke WA, Granzier H. A spring tale: new facts on titin elasticity. *Biophys J*. 1998;75:2613–2614.
3. Granzier HL, Irving TC. Passive tension in cardiac muscle: contribution of collagen, titin, microtubules, and intermediate filaments. *Biophys J*. 1995;68:1027–1044.
4. Linke WA, Ivemeyer M, Olivieri N, Kolmerer B, Rüegg JC, Labeit S. Towards a molecular understanding of the elasticity of titin. *J Mol Biol*. 1996;261:62–71.
5. Trombitas K, Greaser M, Labeit S, Jin JP, Kellermayer M, Helmes M, Granzier H. Titin extensibility in situ: entropic elasticity of permanently folded and permanently unfolded molecular segments. *J Cell Biol*. 1998; 140:853–859.
6. Labeit S, Kolmerer B. Titins, giant proteins in charge of muscle ultrastructure and elasticity. *Science*. 1995;270:293–296.
7. Linke WA, Ivemeyer M, Mundel P, Stockmeier MR, Kolmerer B. Nature of PEVK-titin elasticity in skeletal muscle. *Proc Natl Acad Sci U S A*. 1995;95:8052–8057.
8. Linke WA, Rudy DE, Centner T, Gautel M, Witt CC, Labeit S, Gregorio CC. I-band titin in cardiac muscle is a three-element molecular spring and is critical for maintaining thin filament structure. *J Cell Biol*. 1999;246: 631–644.
9. Helmes M, Trombitas K, Centner T, Kellermayer M, Labeit S, Linke WA, Granzier H. Mechanically driven contour-length adjustment in rat cardiac titin's unique N2B sequence: titin is an adjustable spring. *Circ Res*. 1999;84:1339–1352.
10. Hu DH, Kimura S, Maruyama K. Sodium dodecyl sulfate gel electrophoresis studies of connectin-like high molecular weight proteins of various types of vertebrate and invertebrate muscles. *J Biochem (Tokyo)*. 1986;99:1485–1492.
11. Wang K, McCarter R, Wright J, Beverly J, Ramirez-Mitchell R. Regulation of skeletal muscle stiffness and elasticity by titin isoforms: a test of the segmental extension model of resting tension. *Proc Natl Acad Sci U S A*. 1991;88:7101–7105.
12. Horowits R. Passive force generation and titin isoforms in mammalian skeletal muscle. *Biophys J*. 1992;61:392–398.
13. Cazorla O, Freiburg A, Helmes M, Centner T, McNabb M, Trombitas K, Labeit S, Granzier H. Differential expression of cardiac titin isoforms and modulation of cellular stiffness. *Circ Res*. 2000;86:59–67.
14. Rossi E, Faiella A, Zeviani M, Labeit S, Floridia G, Brunelli S, Cammarata M, Boncinelli E, Zuffardi O. Order of six loci at 2q24–q31 and orientation of the HOXD locus. *Genomics*. 1994;24:34–40.
15. Brady AJ. Length dependence of passive stiffness in single cardiac myocytes. *Am J Physiol*. 1991;260:H1062–H1071.
16. Fabiato A, Fabiato F. Myofilament-generated tension oscillations during partial calcium activation and activation dependence of the sarcomere length-tension relation of skinned cardiac cells. *J Gen Physiol*. 1978;72: 667–699.
17. Greaser ML, Wang S-M, Berri M, Mozdziak PE, Kumazawa Y. Sequence and mechanical implications of cardiac PEVK. In: Pollack GH, Granzier H, eds. *Proceedings: Elastic Filaments of the Cell*. Kluwer Academic/ Plenum Publishers. In press.